Gene expression control by *Bacillus anthracis* purine riboswitches

MARION KIRCHNER and SABINE SCHNEIDER

Center for Integrated Protein Science at the Department of Chemistry, Technische Universität München, 85748 Garching, Germany

ABSTRACT

In all kingdoms of life, cellular replication relies on the presence of nucleosides and nucleotides, the building blocks of nucleic acids and the main source of energy. In bacteria, the availability of metabolites sometimes directly regulates the expression of enzymes and proteins involved in purine salvage, biosynthesis, and uptake through riboswitches. Riboswitches are located in bacterial mRNAs and can control gene expression by conformational changes in response to ligand binding. We have established an inverse reporter gene system in *Bacillus subtilis* that allows us to monitor riboswitch-controlled gene expression. We used it to investigate the activity of five potential purine riboswitches from *Bacillus anthracis* in response to different purines and pyrimidines. Furthermore, in vitro studies on the aptamer domains of the riboswitches reveal their variation in guanine binding affinity ranging from namomolar to micromolar. These data do not only provide insight into metabolite sensing but can also aid in engineering artificial cell regulatory systems.

Keywords: purine riboswitches; *Bacillus anthracis*; purine biosynthesis; nucleobase salvage; nucleotide metabolism

INTRODUCTION

Riboswitches are structural elements in the 5′ untranslated region of mRNAs, which consist of an aptamer domain and an expression platform (Fig. 1; Mandal et al. 2003). They are able to respond to a variety of metabolites, e.g., some amino acids, purines, cofactors, or metals, and due to their high ligand specificity they can be grouped according to the metabolite they recognize (for review, see Serganov and Nudler 2013). In general, ligand binding to the aptamer domain of the riboswitch induces a conformational change and modulation of transcription or translation. Translational riboswitches control gene expression by regulating the accessibility of the ribosome binding site or the start codon. In contrast, ligand binding to transcription-regulating riboswitches leads to the formation of a ρ-independent terminator, which inhibits elongation by destabilizing the RNA–RNA polymerase complex (Bastet et al. 2011). In addition, riboswitches exert gene expression control also by other mechanisms: Recently, a dual-acting lysine riboswitch was identified in *Escherichia coli*, which does not only control initiation of translation but also mRNA decay (Caron et al. 2012). Other riboswitches act through metabolite-dependent alternative 3′-end processing of mRNA or through an intrinsic ribozyme activity in response to ligand binding and riboswitch folding (Cheah et al. 2007; Collins et al. 2007; Wachter et al. 2007). Riboswitches are already known to be targeted by some antibacterial compounds, e.g., by L-aminoethylcysteine or roseoflavin (Blount et al. 2007; Ott et al. 2009). Another compound that targets flavin mononucleotide (FMN) riboswitches was shown to inhibit bacterial growth in a murine model (Blount et al. 2015).

In general, bacteria utilize riboswitches to directly link the abundance of metabolites to the expression of genes responsible for their biosynthesis or transport (Tucker and Breaker 2005; Montange and Batey 2008). For example, expression of the xanthine phosphoribosyl transferase (Xpt), which is involved in nucleoside metabolism, is controlled by the guanine-binding *xpt* riboswitch in *B. subtilis* (Christiansen et al. 1997). Nucleosides are essential metabolites for all organisms as energy donors and building blocks for RNA and DNA. Generally, nucleobases can be synthesized by two means: de novo starting from 5-phosphoribosyl-α-1-pyrophosphate (PRPP); or by salvage pathways initiated from internal and external nucleotides, nucleosides, or nucleobases (Kappock et al. 2000; Switzer et al. 2002; Wolff et al. 2007; Zhang et al. 2008; Belitsky and Sonenshein 2011). The salvage pathways can be used to compensate defects in the de novo

Corresponding authors: marion.kirchner@tum.de, sabine.schneider@mytum.de

Article is online at http://www.rnajournal.org/cgi/doi/10.1261/rna.058792.116.

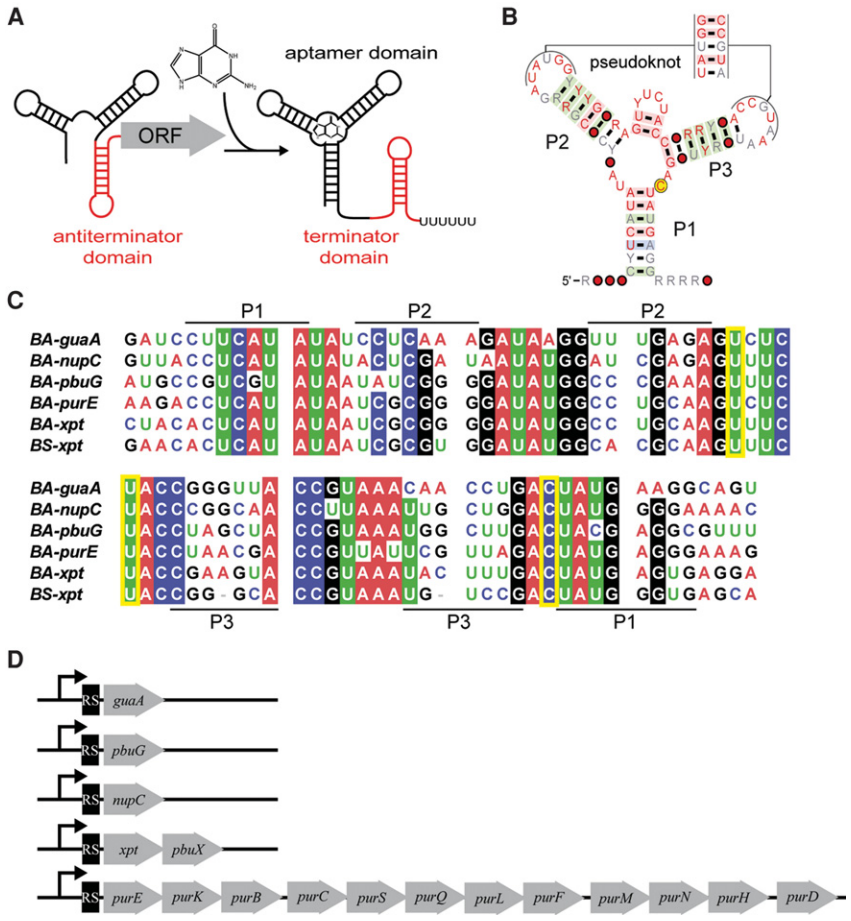

FIGURE 1. Schematic representation of a guanine riboswitch and sequence conservation. (*A*) Binding of guanine to the aptamer domain (black) triggers a conformational change of the anti-terminator domain (red, *left*) to form a transcriptional terminator (red, *right*) (Porter et al. 2014). (*B*) Consensus structure of the aptamer domains of the *B. anthracis* guanine riboswitches. The cytosine forming a Watson–Crick base pair with the guanine is labeled by a yellow circle. Red circles represent nucleotides present in all riboswitches (97%). The nucleotide identity is depicted by light gray (75%; i.e., true for four out of five riboswitches) and red (97%; i.e., in all riboswitches) characters. Green, blue, or red-shaded base pairs indicate covarying, compatible, or conserved nucleobases: R = A or G; Y = C or U. The possible pseudoknot formed upon ligand binding is indicated on *top* of the structure. The schematic representation was generated with the software R2R (Weinberg and Breaker 2011). (*C*) Sequence alignment of the aptamer domains of five *B. anthracis* guanine riboswitches and the *B. subtilis xpt* riboswitch. Nucleobases conserved in five of the six sequences are shaded. Residues belonging to the helices P1, P2, or P3 of the *B. subtilis xpt* aptamer domain are indicated. Framed in yellow are the conserved cytosine and two uracil bases making direct contacts with the purine in the X-ray crystal structure of the *BS-xpt* aptamer (PDB code 1Y27) (Serganov et al. 2004). (*D*) Schematic representation of genes (gray arrows) and operons regulated by guanine riboswitches (RS; black box) investigated here. Genomic localizations in *B. anthracis* strain Ames according to MicrobesOnline (Dehal et al. 2010); references correspond to the *B. subtilis* analogs of the genes. *guaA* (GMP synthase; BA0268) (Mantsala and Zalkin 1992); *pbuG* (hypoxanthine-guanine permease; BA0270) (Saxild et al. 2001); *nupC* (nucleoside transporter; BA0332) (Saxild et al. 1996); *xpt* (xanthine phosphoribosyltransferase; BA1591) (Christiansen et al. 1997); *pbuX* (xanthine permease; BA1592) (Christiansen et al. 1997); *purE* (phosphoribosylaminoimidazole carboxylase BA0288) (Johansen et al. 2003); *purK* (phosphoribosylaminoimidazole carboxylase BA0289) (Johansen et al. 2003); *purB* (adenylsuccinate lyase; BA0290); *purC* (phosphoribosylaminoimidazole succinocarboxamide synthase; BA0291); *purS* (phosphoribosylformylglycinamidine synthase; BA0292); *purQ* (phosphoribosylformylglycinamidine synthase; BA0293); *purL* (phosphoribosylformylglycinamidine synthase; BA0294): *purF* (glutamine phosphoribosyldiphosphate amidotransferase; BA0295); *purM* (phosphoribosylaminoimidazole synthase; BA0296); *purN* (phosphoribosylglycinamide formyltransferase; BA0297); *purH* (phosphoribosylaminoimidazole carboxamide formyltransferase; BA0298); *purD* (phosphoribosylglycinamide synthetase; BA0299) (Ebbole and Zalkin 1987; Johansen et al. 2003).

purine synthesis. Purine biosynthesis is essential for virulence as well as for growth of a number of pathogenic bacteria, such as *Staphylococcus aureus* (Mei et al. 1997; Kofoed et al. 2016), *Yersinia pestis* (Brubaker 1970), and *B. anthracis* (Jenkins et al. 2011). This can be exploited for drug design; e.g., inhibitors of the N^5-carboxyaminoimidazole ribonucleotide (CAIR) mutase PurE exhibited antimicrobial activity against *B. anthracis* (Kim et al. 2015). In addition, an *xpt* riboswitch agonist was shown to inhibit *S. aureus* growth in a murine model. However, its antibiotic activity cannot only be traced back to riboswitch binding (Mulhbacher et al. 2010; Kofoed et al. 2016).

To verify the activity of five potential purine riboswitches in *B. anthracis* whose aptamer domains were proposed in 2007 (Barrick and Breaker 2007), we established an in vivo reporter gene system in *B. subtilis* that allows us to directly monitor their gene regulatory function in response to the presence of ligands. We show that these sequences indeed act as riboregulators and shut down gene expression in a dose-dependent manner, specifically in response to guanine but not adenine. Furthermore, we confirmed and analyzed the binding of guanine to the aptamer domains in vitro, revealing their differences in the dissociation constants ranging from 50 nM to 4 μM. Our study provides insights into the function of these important regulators and could aid in utilizing them as gene-regulatory tools and sensors in genetic circuits.

RESULTS

Using the aptamer domains identified by Barrick and Breaker (2007) as well as the genomic location, we chose five potential *B. anthracis* guanine riboswitches, which are likely to regulate the expression of genes related to purine biosynthesis, transport, and salvage. According to the first gene downstream from their genomic location, they are called *guaA*, *nupC*, *pbuG*, *purE*, and *xpt* here (Fig. 1; Barrick and Breaker 2007; Singh and Sengupta 2012). Sequence and secondary

structure analysis of the expression platforms of these potential five *B. anthracis* riboswitches revealed putative ρ-independent terminators. Therefore, we assume that they act through a transcription attenuation mechanism (Barrick and Breaker 2007). To analyze these putative riboswitches, we developed a novel inverse reporter gene system: We cloned their sequences (starting 10 bases 5′ of the P1 stems of predicted aptamer domains and ending directly before the ribosome binding site) between a xylose-responsive promoter (P_{xyl}) and *blaI*, a gene encoding for a transcriptional repressor. To exclude the impact of translation initiation efficiency, we used the same optimal *B. subtilis* ribosome binding site for all constructs (Vellanoweth and Rabinowitz 1992; Ma et al. 2002). The transcriptional repressor BlaI, in turn, regulates the activity of a promoter called P_{blaP} (Grossman et al. 1989) and thereby inhibits the expression of a downstream luciferase operon (*luxABCDE*) (Fig. 2A). With this reverse reporter system, we can monitor riboswitch-mediated inhibition of gene expression as an increase in bioluminescence. Single copies of all expression constructs were integrated into the *B. subtilis* W168 genome.

If cloned without any riboswitch (Δ RS), BlaI reduces *luxABCDE* expression upon xylose induction independently of guanosine presence to the wild-type (W168) level (Fig. 2B). Guanosine was used here for in vivo assays instead of guanine because of its higher water solubility. It is taken up by *B. subtilis* nucleoside transporters like NupNOPQ or NupG and converted intracellularly into the active compound guanine by PupG (Schuch et al. 1999; Johansen et al. 2003; Belitsky and Sonenshein 2011). Addition of xylose to the strain containing the well-characterized *B. subtilis xpt* riboswitch (Mulhbacher and Lafontaine 2007) (*BS-xpt*) also clearly decreases bioluminescence (Fig. 2B, white and striped bars). When the medium is supplemented with xylose and guanosine, we observe an about 60-fold increase in bioluminescence (Fig. 2B, black bars). This demonstrates that our in vivo reporter system is well suited to characterize the gene regulatory function of riboswitches. Next, we investigated the potential *B. anthracis xpt* (*BA-xpt*) riboswitch. As in *B. subtilis*, this predicted riboswitch is located upstream of an operon containing the genes

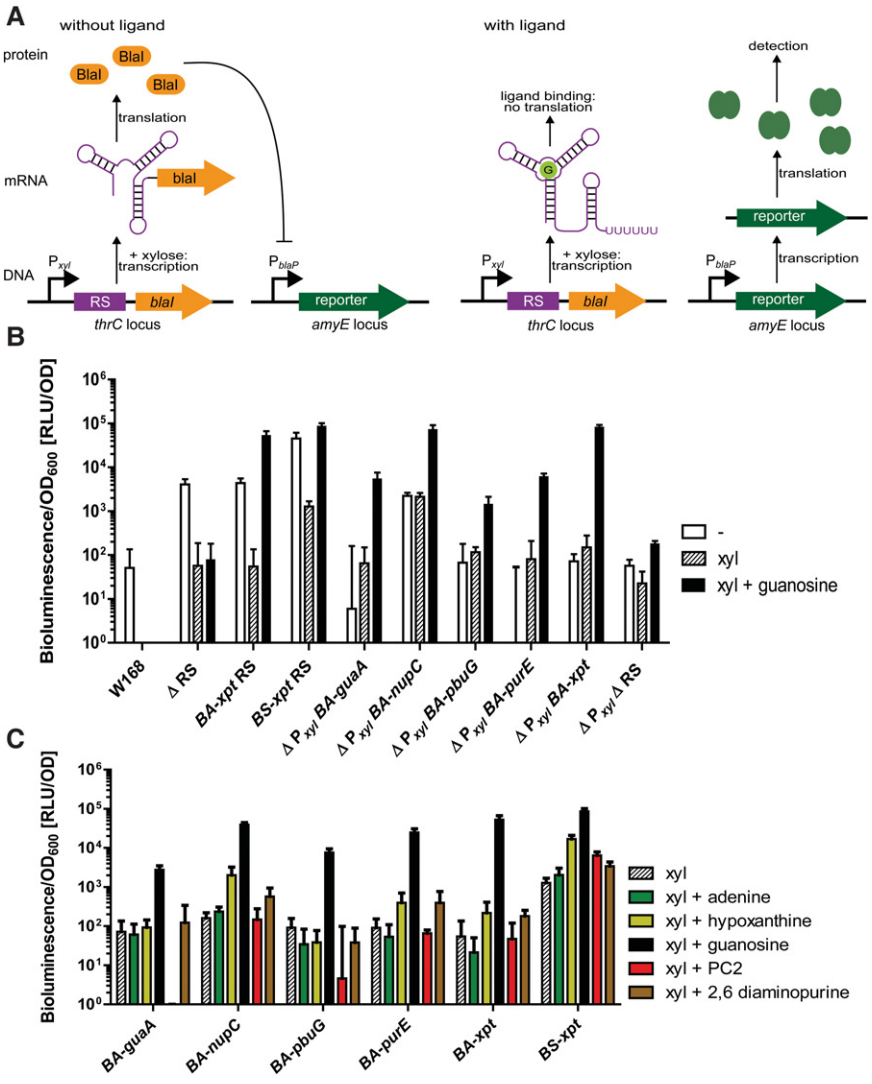

FIGURE 2. Reverse reporter gene system and gene regulation by purine riboswitches in *B. subtilis*. (*A*) Scheme of the reverse reporter gene system. The target riboswitch (purple) regulates the expression of *blaI* (orange). BlaI controls the luciferase reporter genes *luxABCDE* (green) through P_{blaP}. (*Left*) If no riboswitch ligand is present, P_{blaP} is inhibited and no reporter gene activity can be detected. (*Right*) Ligand binding to the riboswitch leads to down-regulation of BlaI, thereby creating bioluminescence. (*B*) Comparison of the bioluminescence from wild type (W168), the *B. anthracis* and *B. subtilis xpt* riboswitches (*BA-xpt* and BS-*xpt*) as well as controls without P_{xyl} promoter (Δ P_{xyl}), or riboswitch (Δ RS), or both (Δ P_{xyl} Δ RS). The relative bioluminescence was determined without (white bars) and with addition of xylose (xyl; striped bars) as well as with xylose and 1 mM guanosine (black bars). (*C*) Response of the *B. anthracis guaA*, *nupC*, *pbuG*, *purE*, and *xpt* riboswitches and the *B. subtilis xpt* riboswitch to guanosine (black bars), adenine (green bars), hypoxanthine (light green bars), PC2 (red bars), and 2,6-diaminopurine (brown bars). For simplicity, all riboswitches are named according to the first gene in the operon they regulate. If the gene is not yet annotated in the genome database, it is named according to its homolog in *B. subtilis* W168 (BA0270: 65.7% homology with PbuG; BA0332: 42.2% homology with NupC). The bioluminescence was measured 3.3 h after induction with xylose and addition of guanosine, adenine etc., normalized by the cell density (OD_{600}) and plotted on a logarithmic scale in RLU/OD. The standard deviations of three independent experiments are indicated by error bars. *BA* = *B. anthracis*, *BS* = *B. subtilis*, RS = riboswitch. Note: Due to its higher solubility in the medium, guanosine instead of guanine was used. W168 denotes the wild-type *B. subtilis* strain W168, showing the cellular background level.

xpt and *pbuX* in the *B. anthracis* genome and shares 69.6% sequence identity and 63.1% similarity with the *B. subtilis xpt* riboswitch aptamer domain (Fig. 1C,D). Upon guanosine addition, the strain containing the *BA-xpt* riboswitch construct displays an about 10^3-fold increased bioluminescence in comparison to the xylose-containing sample, showing that this RNA sequence indeed controls gene expression (Fig. 2B). Furthermore, the other four predicted guanine riboswitches from *B. anthracis* regulate gene expression also in a guanosine-dependent manner. For the highest guanosine concentration, inductions between 40- and 10^3-fold were observed (Fig. 2C). As a control we also removed the promoter P_{xyl} in front of the riboswitches (ΔP_{xyl}). The corresponding strains show similar luminescence values with and without xylose (Fig. 2B), indicating transcriptional read-through from the P_{hom}-promoter located upstream of the genomic *thrC* integration site. Nevertheless, they still exhibit a clear response upon guanosine addition with and without xylose (Fig. 2B, black bars), highlighting the function of the reporter system.

Addition of hypoxanthine to the media leads to activation of the *BA-nupC*, *BA-purE*, and both *xpt*-riboswitches, although the increase of reporter gene expression is small compared to guanosine. No alteration in bioluminescence is observed when the media is supplemented with adenine (Fig. 2C). This shows that the gene-regulatory function of these riboswitches is specific to guanosine and, in part, to hypoxanthine, but not to adenine (Fig. 2C). Furthermore, it again confirms the so-called G-box, a unique feature of guanine riboswitches, with an essential cytosine (C) forming a Watson–Crick base pair with the guanine ligand (Batey et al. 2004; Gilbert et al. 2006). The five *B. anthracis* riboswitches investigated here all possess this crucial C (Fig. 1), in contrast to adenine-responsive riboswitches which carry a uracil (U) at the equivalent position (Serganov et al. 2004; Lemay et al. 2006; Lemay and Lafontaine 2007). In addition, the *B. anthracis* riboswitches also contain the two U bases, which make direct contacts with the purine in the X-ray crystal structure of the *BS-xpt* aptamer (PDB code 1Y27) (Serganov et al. 2004). Moreover, their gene regulatory function is linked to the amount of guanosine present in the media as we observe a direct dose-dependent correlation between guanosine concentration and increase of bioluminescence in our reporter system (Fig. 3). However, the efficiency of different *B. anthracis* riboswitches to shut down gene expression in the presence of guanosine varies and ranges, e.g., for 250 µM guanosine from about 30% to 70% of the maximal observed bioluminescence read-out. Similar dose-response effects have been observed in a previous study on three guanine riboswitches of *B. subtilis* (Mulhbacher and Lafontaine 2007).

A work on the *BS-xpt* riboswitch showed that the pyrimidine analogs 2,5,6-triaminopyrimidin-4-one (PC1) and 2,6-diaminopyrimidin-4-one (PC 2) bind to the *BS-xpt* aptamer (Mulhbacher et al. 2010). In our in vivo system we see a statistical significant increase in reporter gene expression upon addition of PC2 only for the *BS-xpt* riboswitch, but not for any of the *B. anthracis* riboswitches (Fig. 2C). Our reporter strains displayed considerable growth defects upon PC1 treatment, which hinders the determination of reporter gene expression levels with this compound (data not shown). We also tested another purine analog (2,6-diaminopurine), which only activated the *BA-nupC* riboswitch, but has no impact on any other riboswitch (Fig. 2C). Our results again highlight the specific nature of the riboswitch aptamers.

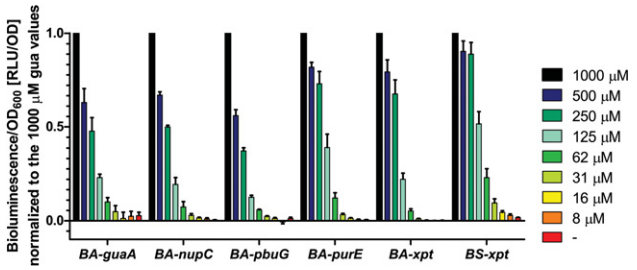

FIGURE 3. Dose-dependent gene regulation by *B. subtilis xpt* and *B. anthracis* guanine riboswitches. The bioluminescence measured for 1000 µM guanosine (gua) was divided by the cell density (OD_{600}) and set to one (100%). The bioluminescence/OD_{600} values for the samples supplemented with 0–500 µM guanosine are normalized to the 1000 µM guanosine values. The bioluminescence was determined 3.3 h after induction with the same amount of xylose and varying guanosine concentrations.

In order to determine the dissociation constants of ligand binding to the riboswitches, we generated fusion-RNAs by in vitro transcription, where the aptamer domains of the purine riboswitches were fused with their respective P1-stem to the P2-stem of the Spinach2 aptamer. Thus, fluorescence of the Spinach2 aptamer upon 3,5-difluoro-4-hydroxybenzylidene imidazolinone (DFHBI)-binding is dependent on ligand binding to the riboswitch aptamer (Kellenberger and Hammond 2015). This assay can be used to determine dissociation constants by measuring the fluorescence in the presence of varying ligand concentrations. For all riboswitches the dissociation constants K_D for guanine range over two orders of magnitude from 50 nM to 4 µM, with the *xpt* riboswitches from *B. anthracis* and *B. subtilis* exhibiting the strongest binding affinity ($K_D \approx 50$ nM) in our assay conditions (Table 1).

DISCUSSION

Nucleosides and nucleotides are essential for every organism. In *B. anthracis*, potential purine riboswitch sequences are found in the 5′ UTR of genes and operons encoding for enzymes involved in purine de novo synthesis, uptake, and salvage, possibly linking the abundance of purines to gene expression control. We have established a reverse reporter gene system that transposes transcriptional inhibition through the action of riboswitches in a positive bioluminescence signal. The single-copy genomic integration of the two parts of the reporter system (P_{xyl}-RS-*blaI*; P_{blaP}-*luxABCDE*)

TABLE 1. Dissociation constants of guanine binding to the purine riboswitch aptamer domains determined by fusion of the aptamer domains to the Spinach2-aptamer and measuring the fluorescence (absorption: 457 nm; emission: 503 nm) (Kellenberger and Hammond 2015)

	K_D (μM)	ΔG^{Term}
BA-guaA	4.10 (±3.72)	−26.4
BA-nupC	0.27 (±0.12)	−28.7
BA-pbuG	1.19 (±0.33)	−12.7
BA-purE	3.52 (±1.22)	−25.9
BA-xpt	0.04 (±0.01)	−32.1
BS-xpt	0.05 (±0.01)	−23.0

The relative free energies of the terminator stems (ΔG^{Term}) were calculated using the program Mfold (Zuker 2003), without taking possible tertiary interactions into account.

avoids impact from different copy numbers. Nevertheless, the incorporation of the P_{xyl}-RS-*blaI*-construct in the *thrC* locus poses a challenge because of read-through caused by the P_{hom}-promoter located upstream of the integration site (Radeck et al. 2013). Addition of casamino acids to the medium and cloning a terminator in front of P_{xyl} limits the effect of P_{hom}, but the observed bioluminescence of the strains lacking the P_{xyl} promoter is still lower than expected, indicating residual transcriptional read-through from the P_{hom} promoter. However, in all strains containing a riboswitch, addition of guanosine leads to a significant increase in bioluminescence, independent of the presence of the P_{xyl} promoter (Fig. 2B), thus highlighting the ability of our reporter system to analyze riboswitch function. With this we can also exclude the presence of additional promoters potentially present in the cloned riboswitch sequences, since the Δ P_{xyl} RS strains do not show a lower bioluminescence compared to the Δ P_{xyl} Δ RS control. Other factors such as half-life of the mRNA and BlaI-repressor stability, potential tertiary interactions during terminator formation as well as effects of temperature, local ion, and ligand concentrations will also have an influence on the riboswitch characteristics. Nevertheless, by putting all riboswitches into the same genomic context we are able to assess and compare their gene regulatory function.

With this system we could show that five predicted guanine riboswitches of *B. anthracis* are indeed riboregulators. In the presence of guanosine but not adenine, they shut down gene expression in a specific and dose-dependent manner. Hypoxanthine affected three of out of five *B. anthracis* riboswitches. Another tested nucleoside analog, 2,6-diaminopurine, only weakly activated the *BA-nupC* riboswitch. In addition, only the *BS-xpt* but none of the *B. anthracis* guanine riboswitches studied here responded in our in vivo system to the nucleoside analog PC2, which was previously shown to bind to the *BS-xpt* aptamer (Mulhbacher et al. 2010). This hints at structural differences between the different purine aptamers. By generating aptamer-Spinach2 fusion RNAs we determined the dissociation constants of guanine to the six different aptamer domains and thereby proved that the effects we observe in vivo really are due to the binding of guanine to the riboswitches. The in vitro results vary substantially over two orders of magnitude from 50 nM to about 4 μM, depending on the aptamer (Table 1). The apparent dissociation constants for the binding of guanine to the *BS-xpt* aptamer we observe here is about 10 times lower (≈50 nM) than reported in previous studies (≈5 nM) (Mandal et al. 2003; Mulhbacher and Lafontaine 2007). These differences are likely caused by the different reaction conditions, such as pH, Mg^{2+} concentrations, and temperatures used (40 mM HEPES, pH 7.5, 3 mM $MgCl_2$, 125 mM KCl at 37°C [this study]; 50 mM Tris–HCl, pH 8.0/8.5, 20 mM $MgCl_2$, 100 mM KCl at 25°C [Mandal et al. 2003; Mulhbacher and Lafontaine 2007]), as well as the placement of the guanine aptamers in the context of Spinach2. A similar observation (apparently lower apparent binding affinity for the Spinach2-fusion RNA compared to an in-line probing assay) was previously made by the group of MC Hammond when they compared the dissociation constants for the Vc2-aptamer determined using a Vc2-Spinach2-fusion and an in-line probing assay (Kellenberger et al. 2013). However, by including the previously investigated *BS-xpt* riboswitch in our study we can put our results on the *BA*-riboswitches in relation to previous reports on guanine aptamers.

Comparing the results of our in vitro binding studies and the calculated free energies of the terminator-stem formation (Table 1), we find some correlation to the observed regulatory function of the whole riboswitches in our in vivo reporter gene assay. For the *guaA* riboswitch, for example, we only observed a relatively small, but significant, increase in bioluminescence upon addition of 1 mM guanosine, which is correlated to a low (μM) binding affinity and average stability of the terminator stem. The *pbuG* riboswitch shows the second lowest in vivo activity, which can be explained by an average binding affinity in combination with a very instable terminator. In contrast, the *xpt* and *nupC* riboswitches have aptamer domains with high (nM) binding affinities for guanine and stable terminators, resulting in the high bioluminescence signal in the reporter gene assays. However, the riboswitches investigated here might work by a kinetic rather than a thermodynamic mechanism. Since equilibrium is not reached in the cell, the dissociation constants do not necessarily reflect the biological situation.

In summary, we present an efficient reporter gene system in *B. subtilis* that allows the assessment of riboswitch function in bioluminescence assays in a 96-well format. Due to the inverse character of the system and its single-copy integration into the genome, it is possible to detect binding of high and low affinity ligands efficiently. In combination with the in vitro analysis of ligand binding we provide a detailed characterization of five guanine riboswitches from *B. anthracis*. Our results provide novel insight into the regulatory function of purine-dependent riboswitches and might aid in their use as potential gene-regulatory tools for genetic circuits.

MATERIALS AND METHODS

All chemicals, enzymes, and buffers were purchased from Carl Roth, VWR, AMRESCO, New England Biolabs, or Promega. Synthetic DNA strings encoding for the *B. anthracis* riboswitches and Spinach2-riboswitch fusions were ordered from Thermo Scientific. Bacteria were routinely grown in Luria-Bertani (LB) medium at 37°C with agitation. For plate reader experiments, a modified CSE medium based on MOPS buffer was used [40.0 mM MOPS, 25.0 mM $(NH_4)_2SO_4$, 0.385 mM KH_2PO_4, 0.615 mM K_2HPO_4, 24.5 mM tryptophan, 42.0 mM threonine, 84.0 µM ammonium ferric citrate, 10.4 µM $MnSO_4$, 0.50 mM $MgSO_4$, 43.2 µM potassium glutamate, 37.0 µM sodium succinate, 139 µM fructose, 1% casamino acids] (Commichau et al. 2008; Radeck et al. 2013). The *E. coli* strains DH5α, XL10 gold, or XL1 blue were transformed by electroporation and selected with 100 µg/mL ampicillin. All *B. subtilis* strains are based on W168 and were grown with 100 µg/mL spectinomycin and 5 µg/mL chloramphenicol when appropriate.

Cloning procedures

All riboswitches were cloned under the control of the xylose-inducible promoter P_{xyl} and upstream of the *blaI* repressor from *B. licheniformis* (Brans et al. 2004). BlaI regulates the promoter P_{blaP}, which controls the expression of the luciferase operon *luxABCDE* from *Photorhabdus luminescens*. The two parts of the reporter, P_{xyl}-riboswitch-*blaI* and P_{blaP}-*luxABCDE*, were integrated into the *thrC* locus and the *amyE* locus of the *B. subtilis* strain W168, respectively. All assays were performed in defined medium supplemented with 1% casamino acids for silencing of the *hom-thrC* promoter, which is located upstream of the genomic integration site of our reporter system. In addition, we cloned the sequence of the ρ-independent transcriptional terminator *lysS* (de Saizieu et al. 1997; de Hoon et al. 2005) in front of P_{xyl} to further reduce the potential effects of P_{hom} activity. Xylose and/or nucleosides and analogs were added as appropriate.

Generally, enzymes were used according to manufacturer's instructions. Standard PCRs were performed using Phusion polymerase and Colony-PCRs using GoTaq G2 polymerase. Golden gate cloning was carried out for a scarless insertion of riboswitch parts into a plasmid (Engler et al. 2008, 2009). In brief, plasmid and inserts were amplified with primers containing a BsaI recognition site and the desired restriction site. One plasmid and one insert were incubated with BsaI and a highly concentrated ligase (Roche) in CutSmart (New England Biolabs) buffer for 30 cycles of 37°C for 5 min followed by 20°C for 2 min. The reaction was stored at 4°C until electro-transformation of *E. coli*.

All plasmids were amplified using *E. coli* and isolated with the peqGold Plasmid Miniprep Kit (VWR). They were sequenced by GATC biotech. The transformation of *B. subtilis* was performed as described by Radeck et al. (2013). MNGE-medium (52.1 mM K_2HPO_4, 38.5 mM KH_2PO_4, 2.80 mM sodium citrate, 0.105 M glucose, 10.3 mM potassium glutamate, 39.9 µM ammonium ferric citrate, 233 µM tryptophan, 2.85 mM $MgSO_4$, 399 µM threonine) was inoculated from overnight cultures to an optical density at 600 nm (OD_{600}) of 0.1 and grown at 37°C under agitation until the late logarithmic growth phase. Then, ScaI-linearized plasmids or *B. subtilis* genomic DNA was added to the cells. After 1 h of incubation, 100 µL of a solution containing 2.4% yeast extract, 2.4% casamino acids (CAA), and 1.17 mM tryptophan with 0.387 µM chloramphenicol, if needed, was added, and the cells were incubated for another hour before being plated on LB plates with selection. Integration into the *amyE* locus was verified by iodine starch tests, and for the integration into the *thrC* locus, threonine auxotrophy was tested in minimal medium. For a list of used oligonucleotides and strains see the Supplemental Information.

Computational methods

The riboswitch DNA sequences were taken from *B. anthracis* str. Ames (Read et al. 2003) at MicrobesOnline (Dehal et al. 2010) and the European Bioinformatics Institute (McWilliam et al. 2013; Li et al. 2015). Sequence alignments were done with RNAalifold (Bernhart et al. 2008; Gruber et al. 2008), Clustal Omega (Sievers et al. 2011), and BioEdit (Hall 1999). RNA folding was analyzed using the programs RNAfold (Hofacker 2003) and Mfold (Zuker and Jacobson 1998; Waugh et al. 2002; Zuker 2003). Mfold was also used to determine the Gibbs free energies of the terminators. Figures were generated using the software Prism (ver. 5.0.2, GraphPad), Adobe Illustrator (Adobe), BioEdit, and R2R (Weinberg and Breaker 2011).

Luciferase assays

For luciferase assays, cultures of the strains were grown overnight in LB medium with selection, if appropriate. Day cultures were inoculated 1:100 in modified CSE medium (Commichau et al. 2008; Radeck et al. 2013) and incubated at 37°C and 200 rpm until $OD_{600} \approx 3$ was reached. The cultures were diluted to $OD_{600} = 0.05$ and nucleosides and analogs (final concentration = 0–1 mM) and xylose (0.01% w/v) were added, if necessary. For dose–response curves, 1:2 serial dilutions of guanosine were prepared. One hundred microliters of the cell suspension per well was transferred in a 96-well plate (black, µ-clear, Greiner Bio-One) and bioluminescence and OD_{600} were measured in a Spark 10M multiwell reader (Tecan) using the software SparkControl. The plate was incubated at 37°C with double orbital shaking (108 rpm). Absorbance at 600 nm as well as bioluminescence were measured every 10 min for 16 h. After ~3.3 h (corresponding to the late exponential growth phase), the strongest effect of guanosine and xylose addition was reached. Wells containing medium only were used to blank luminescence and OD_{600}. The relative luminescence units (RLU) were normalized by the measured OD_{600} values resulting in RLU/OD values.

Determination of the binding constants

Binding constants were determined in vitro by fusing the purine riboswitch aptamer domains to the Spinach2 aptamer as previously described (Kellenberger and Hammond 2015). In brief, fusion-RNA constructs, where the P2 stem of the Spinach2 aptamer was replaced with the P1 stem and aptamer domain of the purine riboswitches, were generated by in vitro transcription and purified by denaturing polyacrylamide electrophoresis. In order to efficiently couple 3,5-difluoro-4-hydroxybenzylidene imidazolinone (DFHBI)-binding to the Spinach2 aptamer with ligand binding to the riboswitch aptamers, the P1 stem of the riboswitches was shortened to three base pairs (AUA/UTU) (see Supplemental Table 3). RNA

concentrations were determined by the neutral pH thermal hydrolysis assay to exclude hypochromicity effects from base-pairing (Wilson et al. 2014). In order to determine ligand affinities, RNA was renatured by heating and cooling down to ambient temperatures and mixed with varying ligand concentrations (0–10 μM) in reaction buffer (3 μM final RNA concentration, 40 mM HEPES, pH 7.5, 125 mM KCl, 3 mM $MgCl_2$, 30 μM DFHBI) in 96-well FLUOTRAC 200 plates (Greiner). The reactions were incubated at 37°C and the fluorescence (absorption: 457 nm; emission: 503 nm) was measured in a Spark 10M multiwell reader. When equilibrium was reached, the fluorescence values were blanked using the samples without ligand. Dissociation constants were calculated by fitting the fluorescence values of three independent experiments using the software GraphPad Prism.

SUPPLEMENTAL MATERIAL

Supplemental material is available for this article.

ACKNOWLEDGMENTS

Vectors for *B. subtilis* and protocols were kindly provided by the Mascher laboratory, Technische Universität Dresden. We thank Matthias Stahl for his help with Tecan readers. This work was supported by the Fonds der chemischen Industrie, the Deutsche Forschungsgemeinschaft (DFG SCHN 1273, SFB749, and GRK 2062/1) and the Center for Integrated Protein Science Munich (CIPSM).

Received August 18, 2016; accepted February 12, 2017.

REFERENCES

Barrick JE, Breaker RR. 2007. The distributions, mechanisms, and structures of metabolite-binding riboswitches. *Genome Biol* **8:** R239.

Bastet L, Dubé A, Massé E, Lafontaine DA. 2011. New insights into riboswitch regulation mechanisms. *Mol Microbiol* **80:** 1148–1154.

Batey RT, Gilbert SD, Montange RK. 2004. Structure of a natural guanine-responsive riboswitch complexed with the metabolite hypoxanthine. *Nature* **432:** 411–415.

Belitsky BR, Sonenshein AL. 2011. CodY-mediated regulation of guanosine uptake in *Bacillus subtilis*. *J Bacteriol* **193:** 6276–6287.

Bernhart SH, Hofacker IL, Will S, Gruber AR, Stadler PF. 2008. RNAalifold: improved consensus structure prediction for RNA alignments. *BMC Bioinformatics* **9:** 474.

Blount KF, Wang JX, Lim J, Sudarsan N, Breaker RR. 2007. Antibacterial lysine analogs that target lysine riboswitches. *Nat Chem Biol* **3:** 44–49.

Blount KF, Megyola C, Plummer M, Osterman D, O'Connell T, Aristoff P, Quinn C, Chrusciel RA, Poel TJ, Schostarez HJ, et al. 2015. Novel riboswitch-binding flavin analog that protects mice against *Clostridium difficile* infection without inhibiting cecal flora. *Antimicrob Agents Chemother* **59:** 5736–5746.

Brans A, Filée P, Chevigné A, Claessens A, Joris B. 2004. New integrative method to generate *Bacillus subtilis* recombinant strains free of selection markers. *Appl Environ Microbiol* **70:** 7241–7250.

Brubaker RR. 1970. Interconversion of purine mononucleotides in *Pasteurella pestis*. *Infect Immun* **1:** 446–454.

Caron MP, Bastet L, Lussier A, Simoneau-Roy M, Massé E, Lafontaine DA. 2012. Dual-acting riboswitch control of translation initiation and mRNA decay. *Proc Natl Acad Sci* **109:** E3444–E3453.

Cheah MT, Wachter A, Sudarsan N, Breaker RR. 2007. Control of alternative RNA splicing and gene expression by eukaryotic riboswitches. *Nature* **447:** 497–500.

Christiansen LC, Schou S, Nygaard P, Saxild HH. 1997. Xanthine metabolism in *Bacillus subtilis*: characterization of the *xpt-pbuX* operon and evidence for purine- and nitrogen-controlled expression of genes involved in xanthine salvage and catabolism. *J Bacteriol* **179:** 2540–2550.

Collins JA, Irnov I, Baker S, Winkler WC. 2007. Mechanism of mRNA destabilization by the *glmS* ribozyme. *Genes Dev* **21:** 3356–3368.

Commichau FM, Gunka K, Landmann JJ, Stülke J. 2008. Glutamate metabolism in *Bacillus subtilis*: gene expression and enzyme activities evolved to avoid futile cycles and to allow rapid responses to perturbations of the system. *J Bacteriol* **190:** 3557–3564.

Dehal PS, Joachimiak MP, Price MN, Bates JT, Baumohl JK, Chivian D, Friedland GD, Huang KH, Keller K, Novichkov PS, et al. 2010. MicrobesOnline: an integrated portal for comparative and functional genomics. *Nucleic Acids Res* **38:** D396–D400.

de Hoon MJ, Makita Y, Nakai K, Miyano S. 2005. Prediction of transcriptional terminators in *Bacillus subtilis* and related species. *PLoS Comput Biol* **1:** e25.

de Saizieu A, Vankan P, Vockler C, van Loon AP. 1997. The *trp* RNA-binding attenuation protein (TRAP) regulates the steady-state levels of transcripts of the *Bacillus subtilis* folate operon. *Microbiology* **143** (Pt 3): 979–989.

Ebbole DJ, Zalkin H. 1987. Cloning and characterization of a 12-gene cluster from *Bacillus subtilis* encoding nine enzymes for de novo purine nucleotide synthesis. *J Biol Chem* **262:** 8274–8287.

Engler C, Kandzia R, Marillonnet S. 2008. A one pot, one step, precision cloning method with high throughput capability. *PLoS One* **3:** e3647.

Engler C, Gruetzner R, Kandzia R, Marillonnet S. 2009. Golden gate shuffling: a one-pot DNA shuffling method based on type IIs restriction enzymes. *PLoS One* **4:** e5553.

Gilbert SD, Stoddard CD, Wise SJ, Batey RT. 2006. Thermodynamic and kinetic characterization of ligand binding to the purine riboswitch aptamer domain. *J Mol Biol* **359:** 754–768.

Grossman MJ, Curran IH, Lampen JO. 1989. Interaction of BlaI, the repressor for the β-lactamase gene of *Bacillus licheniformis*, with the *blaP* and *blaI* promoters. *FEBS Lett* **246:** 83–88.

Gruber AR, Lorenz R, Bernhart SH, Neubock R, Hofacker IL. 2008. The Vienna RNA websuite. *Nucleic Acids Res* **36:** 70–74.

Hall TA. 1999. BioEdit: a user-friendly biological sequence alignment editor and analysis program for Windows 95/98/NT. *Nucleic Acids Symposium Series* **41:** 95–98.

Hofacker IL. 2003. Vienna RNA secondary structure server. *Nucleic Acids Res* **31:** 3429–3431.

Jenkins A, Cote C, Twenhafel N, Merkel T, Bozue J, Welkos S. 2011. Role of purine biosynthesis in *Bacillus anthracis* pathogenesis and virulence. *Infect Immun* **79:** 153–166.

Johansen LE, Nygaard P, Lassen C, Agerso Y, Saxild HH. 2003. Definition of a second *Bacillus subtilis pur* regulon comprising the *pur* and *xpt-pbuX* operons plus *pbuG*, *nupG* (*yxjA*), and *pbuE* (*ydhL*). *J Bacteriol* **185:** 5200–5209.

Kappock TJ, Ealick SE, Stubbe J. 2000. Modular evolution of the purine biosynthetic pathway. *Curr Opin Chem Biol* **4:** 567–572.

Kellenberger CA, Hammond MC. 2015. *In vitro* analysis of riboswitch-Spinach aptamer fusions as metabolite-sensing fluorescent biosensors. *Methods Enzymol* **550:** 147–172.

Kellenberger CA, Wilson SC, Sales-Lee J, Hammond MC. 2013. RNA-based fluorescent biosensors for live cell imaging of second messengers cyclic di-GMP and cyclic AMP-GMP. *J Am Chem Soc* **135:** 4906–4909.

Kim A, Wolf NM, Zhu T, Johnson ME, Deng J, Cook JL, Fung LW. 2015. Identification of *Bacillus anthracis* PurE inhibitors with antimicrobial activity. *Bioorg Med Chem* **23:** 1492–1499.

Kofoed EM, Yan D, Katakam AK, Reichelt M, Lin B, Kim J, Park S, Date SV, Monk IR, Xu M, et al. 2016. *De novo* guanine biosynthesis but not the riboswitch-regulated purine salvage pathway is required

for *Staphylococcus aureus* infection *in vivo*. *J Bacteriol* **198:** 2001–2015.

Lemay JF, Lafontaine DA. 2007. Core requirements of the adenine riboswitch aptamer for ligand binding. *RNA* **13:** 339–350.

Lemay JF, Penedo JC, Tremblay R, Lilley DM, Lafontaine DA. 2006. Folding of the adenine riboswitch. *Chem Biol* **13:** 857–868.

Li W, Cowley A, Uludag M, Gur T, McWilliam H, Squizzato S, Park YM, Buso N, Lopez R. 2015. The EMBL-EBI bioinformatics web and programmatic tools framework. *Nucleic Acids Res* **43:** W580–W584.

Ma J, Campbell A, Karlin S. 2002. Correlations between Shine-Dalgarno sequences and gene features such as predicted expression levels and operon structures. *J Bacteriol* **184:** 5733–5745.

Mandal M, Boese B, Barrick JE, Winkler WC, Breaker RR. 2003. Riboswitches control fundamental biochemical pathways in *Bacillus subtilis* and other bacteria. *Cell* **113:** 577–586.

Mantsala P, Zalkin H. 1992. Cloning and sequence of *Bacillus subtilis purA* and *guaA*, involved in the conversion of IMP to AMP and GMP. *J Bacteriol* **174:** 1883–1890.

McWilliam H, Li W, Uludag M, Squizzato S, Park YM, Buso N, Cowley AP, Lopez R. 2013. Analysis Tool Web Services from the EMBL-EBI. *Nucleic Acids Res* **41:** 597–600.

Mei JM, Nourbakhsh F, Ford CW, Holden DW. 1997. Identification of *Staphylococcus aureus* virulence genes in a murine model of bacteraemia using signature-tagged mutagenesis. *Mol Microbiol* **26:** 399–407.

Montange RK, Batey RT. 2008. Riboswitches: emerging themes in RNA structure and function. *Ann Rev Biophys* **37:** 117–133.

Mulhbacher J, Lafontaine DA. 2007. Ligand recognition determinants of guanine riboswitches. *Nucleic Acids Res* **35:** 5568–5580.

Mulhbacher J, Brouillette E, Allard M, Fortier LC, Malouin F, Lafontaine DA. 2010. Novel riboswitch ligand analogs as selective inhibitors of guanine-related metabolic pathways. *PLoS Pathog* **6:** e1000865.

Ott E, Stolz J, Lehmann M, Mack M. 2009. The RFN riboswitch of *Bacillus subtilis* is a target for the antibiotic roseoflavin produced by *Streptomyces davawensis*. *RNA Biol* **6:** 276–280.

Porter EB, Marcano-Velazquez JG, Batey RT. 2014. The purine riboswitch as a model system for exploring RNA biology and chemistry. *Biochim Biophys Acta* **1839:** 919–930.

Radeck J, Kraft K, Bartels J, Cikovic T, Durr F, Emenegger J, Kelterborn S, Sauer C, Fritz G, Gebhard S, et al. 2013. The Bacillus BioBrick Box: generation and evaluation of essential genetic building blocks for standardized work with *Bacillus subtilis*. *J Biol Eng* **7:** 29.

Read TD, Peterson SN, Tourasse N, Baillie LW, Paulsen IT, Nelson KE, Tettelin H, Fouts DE, Eisen JA, Gill SR, et al. 2003. The genome sequence of *Bacillus anthracis* Ames and comparison to closely related bacteria. *Nature* **423:** 81–86.

Saxild HH, Andersen LN, Hammer K. 1996. *Dra-nupC-pdp* operon of *Bacillus subtilis*: nucleotide sequence, induction by deoxyribonucleosides, and transcriptional regulation by the *deoR*-encoded DeoR repressor protein. *J Bacteriol* **178:** 424–434.

Saxild HH, Brunstedt K, Nielsen KI, Jarmer H, Nygaard P. 2001. Definition of the *Bacillus subtilis* PurR operator using genetic and bioinformatic tools and expansion of the PurR regulon with *glyA*, *guaC*, *pbuG*, *xpt-pbuX*, *yqhZ-folD*, and *pbuO*. *J Bacteriol* **183:** 6175–6183.

Schuch R, Garibian A, Saxild HH, Piggot PJ, Nygaard P. 1999. Nucleosides as a carbon source in *Bacillus subtilis*: characterization of the *drm-pupG* operon. *Microbiology* **145:** 2957–2966.

Serganov A, Nudler E. 2013. A decade of riboswitches. *Cell* **152:** 17–24.

Serganov A, Yuan YR, Pikovskaya O, Polonskaia A, Malinina L, Phan AT, Hobartner C, Micura R, Breaker RR, Patel DJ. 2004. Structural basis for discriminative regulation of gene expression by adenine- and guanine-sensing mRNAs. *Chem Biol* **11:** 1729–1741.

Sievers F, Wilm A, Dineen D, Gibson TJ, Karplus K, Li W, Lopez R, McWilliam H, Remmert M, Soding J, et al. 2011. Fast, scalable generation of high-quality protein multiple sequence alignments using Clustal Omega. *Mol Syst Biol* **7:** 539.

Singh P, Sengupta S. 2012. Phylogenetic analysis and comparative genomics of purine riboswitch distribution in prokaryotes. *Evol Bioinform Online* **8:** 589–609.

Switzer RL, Zalkin H, Saxild HH. 2002. Purine, pyrimidine, and pyridine nucleotide metabolism. In *Bacillus subtilis and its closest relatives*. American Society of Microbiology, Washington, DC.

Tucker BJ, Breaker RR. 2005. Riboswitches as versatile gene control elements. *Curr Opin Struct Biol* **15:** 342–348.

Vellanoweth RL, Rabinowitz JC. 1992. The influence of ribosome-binding-site elements on translational efficiency in *Bacillus subtilis* and *Escherichia coli in vivo*. *Mol Microbiol* **6:** 1105–1114.

Wachter A, Tunc-Ozdemir M, Grove BC, Green PJ, Shintani DK, Breaker RR. 2007. Riboswitch control of gene expression in plants by splicing and alternative 3′ end processing of mRNAs. *Plant Cell* **19:** 3437–3450.

Waugh A, Gendron P, Altman R, Brown JW, Case D, Gautheret D, Harvey SC, Leontis N, Westbrook J, Westhof E, et al. 2002. RNAML: a standard syntax for exchanging RNA information. *RNA* **8:** 707–717.

Weinberg Z, Breaker RR. 2011. R2R - software to speed the depiction of aesthetic consensus RNA secondary structures. *BMC Bioinformatics* **12:** 3.

Wilson SC, Cohen DT, Wang XC, Hammond MC. 2014. A neutral pH thermal hydrolysis method for quantification of structured RNAs. *RNA* **20:** 1153–1160.

Wolff S, Antelmann H, Albrecht D, Becher D, Bernhardt J, Bron S, Buttner K, van Dijl JM, Eymann C, Otto A, et al. 2007. Towards the entire proteome of the model bacterium *Bacillus subtilis* by gel-based and gel-free approaches. *J Chromatogr B Analyt Technol Biomed Life Sci* **849:** 129–140.

Zhang Y, Morar M, Ealick SE. 2008. Structural biology of the purine biosynthetic pathway. *Cell Mol Life Sci* **65:** 3699–3724.

Zuker M. 2003. Mfold web server for nucleic acid folding and hybridization prediction. *Nucleic Acids Res* **31:** 3406–3415.

Zuker M, Jacobson AB. 1998. Using reliability information to annotate RNA secondary structures. *RNA* **4:** 669–679.